Sensors and Materials, Vol. 12, No. 6 (2000) 353–364
MYU Tokyo

S & M 0414

Single-Crystal Silicon Microbolometer and Evaluation of CO_2 Measurement Results

Naoki Kishi, Hara Hitoshi, Nobuhiko Kanbara,
Hideaki Yamagishi[1,*] and Hideto Iwaoka

Corporate R&D Center Micromachining Laboratory, Yokogawa Electric Corporation
2061 Miyada-mura, Kamiina-gun, Nagano Prefecture 399-4394, Japan
[1]Environmental & Analytical Products Business Div. Engineering Dept.,
Yokogawa Electric Corporation
2-9-32 Nakacho, Musashino-shi, Tokyo 180-8750, Japan

(Received July 11, 2000; accepted September 14, 2000)

Key words: uncooled microbolometer, single-crystal silicon, CO_2, NDIR

Single-crystal silicon bolometers fabricated on a silicon-on-insulator (SOI) wafer by bulk micromachining were developed and, using these elements in an NDIR system, CO_2 measurement was investigated. The sensing element of the bolometer functions as both the absorber and the temperature-sensitive resistor. Single-crystal silicon is a suitable material for the microbolometer because the fabrication is compatible with CMOS processes using SOI wafers, the electrical characteristics can be partly controlled by adjusting the impurity concentration, and a microstructure for thermal isolation can be easily achieved. For optimizing detectivity D^* of the bolometer, the temperature coefficient of resistance (TCR), noise voltage and absorptivity of single-crystal silicon for each concentration of impurity were investigated, and the dimensions of the sensing element were designed appropriately. A microbolometer with a specific detectivity of D^*(500 K, 10 Hz, 1 Hz) = 1.1×10^8 cmHz$^{1/2}$/W at a bias voltage of 9.0 V was created. The length of the sensing element was 10 mm. The bolometer was sensitive for wavelengths between 3.5 μm and 8.5 μm. Two bolometers were combined with a micro-variable infrared filter tuned to two different wavelengths: the CO_2 absorption band and the reference band. The two-wavelength nondispersive infrared (NDIR) system for combining these elements with the conventional infrared source could measure the concentration of CO_2 with a reproducibility 3σ of $\pm3.6\%$ of the measured value or less, between concentrations of 0 ppm and 5000 ppm.

*Corresponding author, e-mail address: Naoki_Kishi@yokogawa.co.jp

1. Introduction

In various industries, infrared gas sensing has become feasible for consumer and commercial applications. For example, the use of CO_2 detection systems for home safety and building ventilation control has been steadily increasing. Nondispersive infrared (NDIR) systems that consist of at least an infrared source, an optical filter and a detector are particularly useful for CO_2 sensors. CO_2 has infrared absorption bands at a characteristic wavelength of about 4.25 μm. Absorption increases with concentration according to Lambert-Beer's law, and therefore CO_2 concentration can be measured from the reduction of infrared irradiation of this band. However, the instruments required for NDIR systems are expensive and large, and both the cost and size need to be reduced.

This paper discusses an infrared detector that uses CMOS-compatible materials to meet the demands of reproducibility, uniformity, miniaturization and low cost. At present several kinds of infrared detector are used. Photon detectors need cooling systems at least for the 4.25 μm band. Pyroelectric detectors are also fabricated from unique materials in light of CMOS processes. Thermopile detectors using polysilicon/aluminum[1] have been studied and are commercially available; however, they have complicated structures and are unsuitable for miniaturization and array structures.

At present, resistive thermal detectors, namely bolometers, have been developed as focal plane arrays (FPA) for uncooled thermal imaging by micromachining technology.[2,3] Bolometers are superior to other types of thermal detectors in their simplicity of structure. Microstructures for thermal isolation and the signal processing circuits of FPA are fabricated on an Si substrate by CMOS processing. However, the sensing elements fabricated from materials such as VO_x or Ge[4] having a higher temperature coefficient of resistance (TCR) are fabricated by equipment that is incompatible with CMOS processing. Polysilicon also has a high TCR at low impurity concentration, but its characteristics are closely related to grain size that depends on the deposition conditions.[5]

We selected single-crystal silicon as the material for the bolometer. The absolute value of the temperature coefficient of resistance of single-crystal silicon at room temperature is not as large as that of thermistors. However, using only silicon, this material can be used for all necessary functions of the bolometer: as a temperature sensitive resistor, absorber and thermally isolated structure. The bolometer is characterized by the concentration of impurities such as boron, and the shape and dimensions of the sensing element.

The bolometer was designed to obtain a maximum specific detectivity D^*, so we investigated the concentration of boron in the silicon and discussed factors which affect performance. We fabricated the bolometer on an SOI wafer by bulk micromachining (Fig. 1), and compared measured values with calculated ones.

Finally, we propose an NDIR system using two bolometers and a microvariable infrared filter (MVIF).[6] Both components are fabricated from CMOS compatible materials. The new design allows the system to be produced at low cost, and hence the advantages of NDIR gas sensing may be brought to many applications.

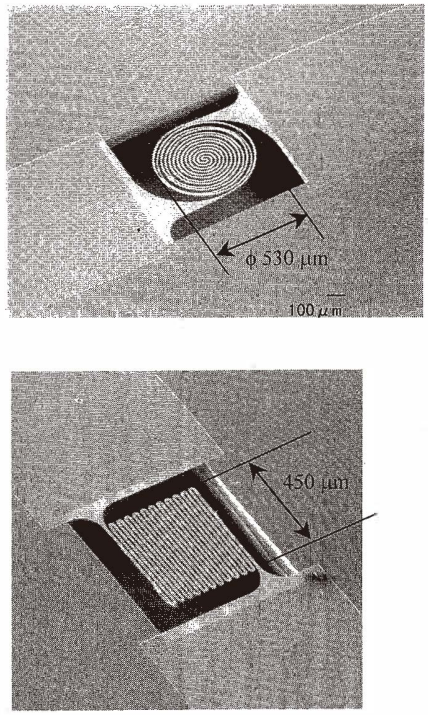

Fig. 1. Scanning electron microscopy photograph of the sensing element of the bolometer: (a) spiral type and (b) meander type. The length, width and thickness of the line are 10 mm, 10 μm and 1.7 μm, respectively. The two bolometers have the same characteristics.

2. Principle

The operation of the bolometer is based upon a change in the electrical resistance of the sensing element due to temperature changes caused by absorbed radiant energy. A bridge circuit and incident radiation modulated by chopping are usually used to detect slight changes in resistance. The specific detectivity D^* is given by eq. (1), where η is the absorptivity for some specific wavelength, V_b the dc bias voltage of the bridge circuit, V_n the noise voltage, Δf the bandwidth of the amplifiers, and f the chopping frequency. The terms α, A, G and C are the TCR, area, thermal conductance and heat capacitance of the sensing element, respectively.

$$D^* = \frac{\eta \alpha V_b}{4GV_n} \sqrt{\frac{\Delta f A}{1+(2\pi f C/G)^2}} \tag{1}$$

3. Design of Impurity Concentration

The variables in eq. (1) are not independent. Especially TCR, the noise voltage and the absorptivity depend on the concentration of boron in silicon, n. These relationships are investigated and an optimum concentration of boron for the bolometer is derived.

The TCR of boron doped single-crystal silicon is positive, 0%/K to 0.8%/K at room temperature, depending only on n as shown in Fig. 2. As the impurity concentration increases, TCR tends to decrease, but in the neighborhood of solid solubility, TCR increases slightly. As for a metal, the relation between resistance and temperature is linear, at least within the range from 300 K to 350 K.

The performance of these detectors is limited by the electrical noise. In this case, the Johnson noise voltage V_j and the $1/f$ noise voltage V_f dominate V_n as shown by eq. (2). The value of V_j depends on the resistance R and the temperature of the bolometer T, as expressed by eq. (3). The term V_f depends on f, the number of charge carriers N, and the voltage across both ends of the bolometer V. Hooge derived the relation between V_f for a bulk semiconductor and these variables by experiment, as given by eq. (4).[7] In this equation, μ represents the mobility of the material, which is a function of n, μL is the mobility due to lattice scattering of p-Si, and a_0 is a constant. As the concentration increases, the mobility decreases and $1/f$ noise also decreases. Hooge's a of boron doped single-crystal silicon was measured and showed the tendency illustrated in Fig. 3. The fact that the experimental values are very scattered could be indicating the inhomogeneous samples and damage to the crystal.

$$V_n^2 = V_j^2 + V_f^2, \tag{2}$$

$$V_j^2 = 4kTR\Delta f, \tag{3}$$

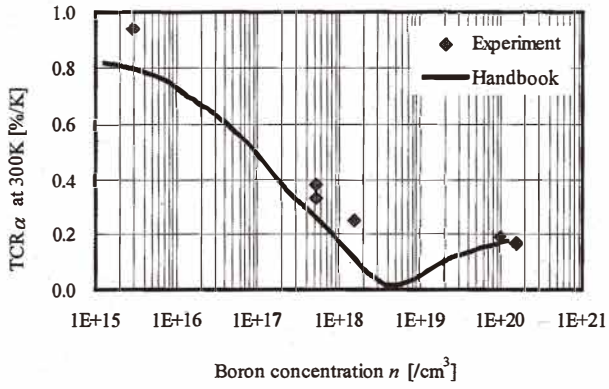

Fig. 2. TCR vs boron concentration of single-crystal silicon.

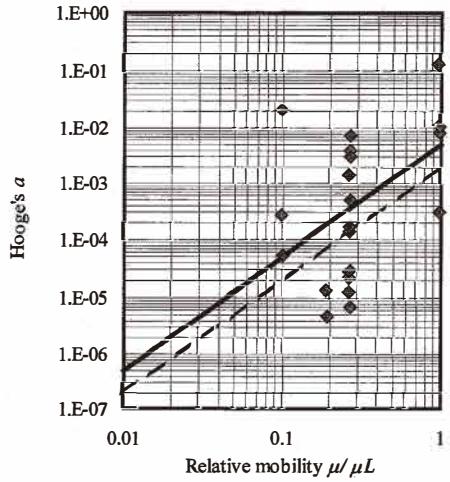

Fig. 3. Relationship between Hooge's a in eq. (4) and the relative mobility. The solid line is the average obtained by experiment. Each sample has a different resistance and the noise voltage is measured at the bias voltage 1.5 V, $\Delta f = 1$ Hz, $f = 10$ Hz. The broken line describes Hooge's results.

$$V_f^2 = \frac{a}{N}\frac{\Delta f}{f}V^2$$

$$a = a_0(\mu / \mu L)^2. \tag{4}$$

Low doped silicon hardly absorbs infrared, except in narrow wavelength bands by silicon lattice absorption. However, highly doped silicon can absorb infrared by free carrier absorption as shown in Fig. 4. The spectra of the absorptivity before and after the silicon substrate was doped with boron are shown in Fig. 5. Note that a doping layer of only 1 μm with a boron concentration of 1×10^{20} /cm^3 vastly improved the absorptivity of silicon. In the region of long wavelengths, the absorptivity decreased because of increased reflectivity. This can be improved by using an anti-reflection coating.

Figure 6 shows the influence of boron concentration in the sensing element upon D^* from Figs. 3 and 4 and eqs. (2), (3), and (4). Figure 6 indicates that for maximum D^* the concentration of boron should be as high as possible.

The electrical noise of the sensing element after fabrication of the bolometer, $n = 1\times10^{20}$ /cm^3, was measured for different bias voltages (Fig. 7), where $R = 20$ kΩ and $\Delta f = 1$ Hz. Using this results, a in eq. (4) was calculated to be 1.2×10^{-3}. This value is larger than that estimated by Hooge. The experimental noise voltage seemed to involve other $1/f$ noise caused by the crystal surface, contacts and circuits.

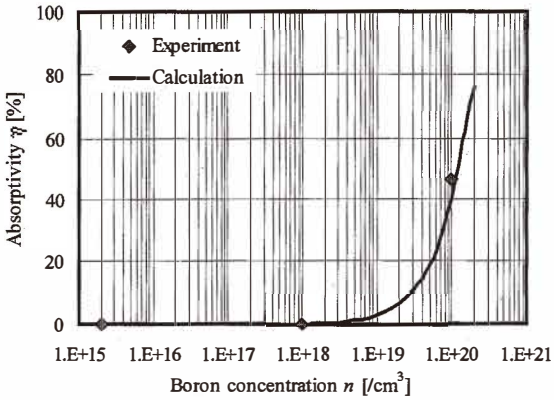

Fig. 4. Relationship between absorptivity and concentration of the boron doped layer at a wavelength $l = 4.25$ μm, a doping depth $d = 1$ μm; for substrate: $n = 2\times10^{15}$ /cm^3, thickness= 525 μm.

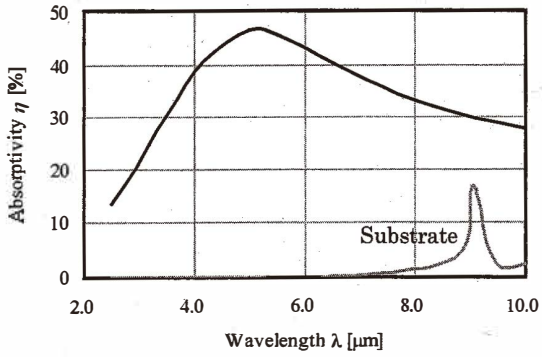

Fig. 5. Spectral absorption of the boron doped layer in silicon. $n = 1\times10^{20}$ /cm^3, doping depth $d =$ 1 μm; substrate: $n = 2\times10^{15}$ /cm^3, thickness= 525 μm.

4. Design of Bolometer

Figure 8 illustrates the process of fabricating the microbolometer. First, the silicon layer of the <100> SOI wafer was doped with boron. Then aluminum electrodes were deposited and formed. In the next step the substrate was etched by anisotropic etching in hydrazine, and SiO_2 is etched. Finally, the sensing element of the bolometer was formed by reactive ion etching.

To minimize the heat capacitance and the thermal conductance, the thermal isolated structure of the sensing element was formed so that highly boron doped single-crystal silicon was suspended from the substrate without other supporters such as a silicon nitride membrane. Single-crystal silicon is an ideal elastic material for forming such a structure.

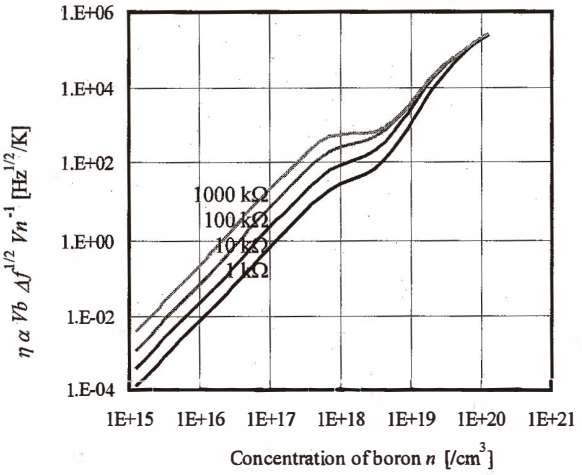

Fig. 6. Influence of boron concentration in the sensing element upon D^*. The vertical line shows the parts of eq. (1) which are influenced by the boron concentration. These values were calculated assuming that $f = 10$ Hz, $\Delta f = 1$ Hz, $T = 300$ K and the power dissipation by V_b is 1 mW.

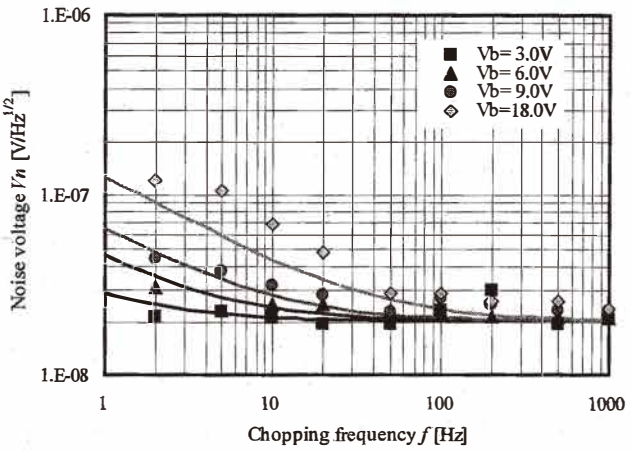

Fig. 7. Spectral noise of the bolometer ($n = 1\times10^{20}$ /cm^3, $R = 20$ kΩ, $\Delta f = 1$ Hz). The solid line shows the calculated value at each V_b using eqs. (2), (3), (4) and $a = 1.2\times10^{-3}$ in eq. (4).

The shape of the sensing element is restricted to the meander type or spiral type, as shown in Fig. 1 due to its low resistivity. If the width and thickness of the sensing element are decided by the demands of the design, the mean thermal conductance can be expressed as

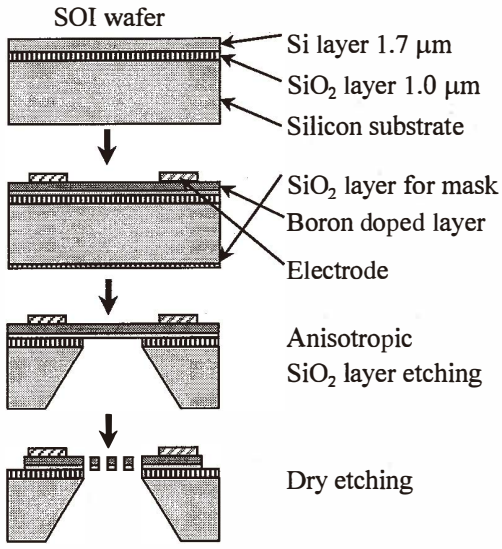

Fig. 8. Process of fabricating the microbolometer.

a function of the length of the sensing element L. As the chopping frequency is decided according to use, D^* is derived as a function of the length of the sensing element L and the dc bias voltage of bridge circuit V_b. Under the two fabrication restrictions, the width of the sensing element w = 10 μm and the thickness of the sensing element d = 1.7 μm, and assuming that the chopping frequency is 10 Hz, D^* is calculated as shown in Fig. 9. The optimum length L = 10 mm and bias voltage V_b = 9.0 V are thus derived. For this length, the resistance equals 20 kΩ.

5. Results

The performance of the bolometer was tested in a vacuum chamber. The radiation source was a blackbody at 500 K. The chamber was closed by a BaF_2 window through which infrared rays irradiated the bolometer. Through the BaF_2 window, the bolometer was sensitive for wavelengths between 3.5 μm and 8.5 μm at half maximum.

By measuring voltage and current, the average thermal conductance was measured to be 4×10^{-6} W/K;[8] its dependence on vacuum pressure is shown in Fig. 10. The calculated heat capacitance is 3×10^{-7} J/K. The value of TCR is 0.2%/K at 300 K, and the total absorptivity calculated from Fig. 5 for a blackbody at 500 K is 48%. The effect of reflection from the package and transmission of the window are taken into account in this value. From these values and the noise voltage in Fig. 7, D^* was calculated. The results of the experiments agree well with the calculated values (Fig. 11).

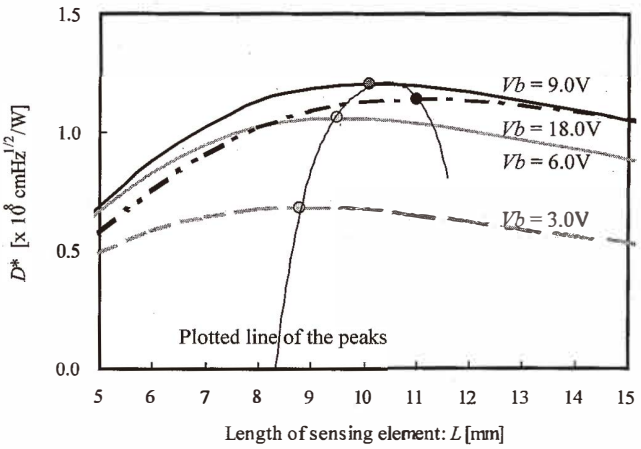

Fig. 9. Specific detectivity D^* (500 K,10 Hz,1 Hz) was calculated to derive an optimum sensing element length L and a bias voltage of the bridge circuit V_b. Note that the maximum D^* (500 K,10 Hz,1 Hz) is obtained when $L = 10$ mm and $V_b = 9.0$ V.

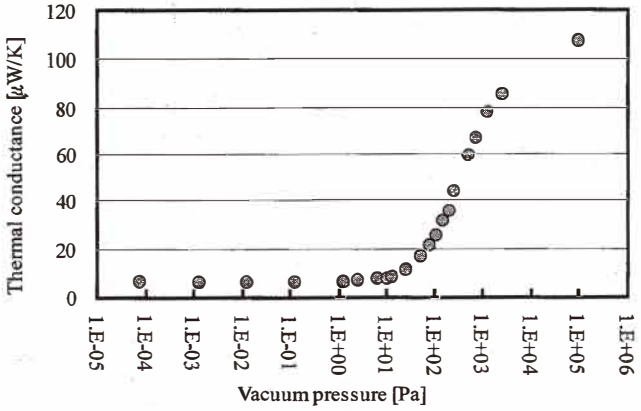

Fig. 10. Relationship between thermal conductance of the sensing element and pressure under vacuum. By measuring voltage and current at each pressure, the average thermal conductance was calculated.[8]

6. CO_2 Measurement

The prototype CO_2 sensor was designed with two microbolometers, an MVIF and an infrared source, as shown in Fig. 12. Generally, the selective infrared linear variable

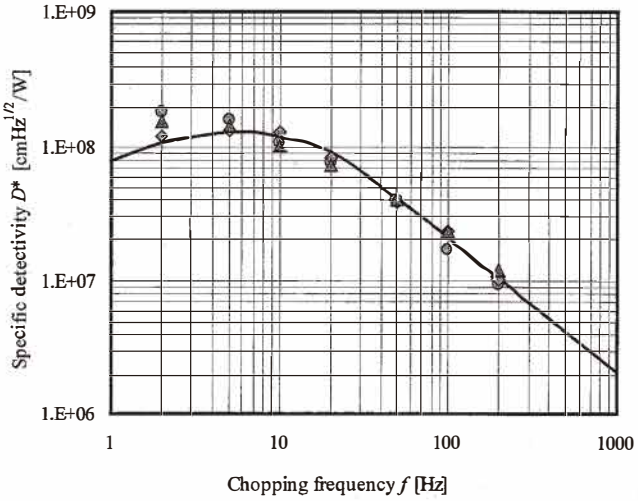

Fig. 11. Comparison between calculations (line) and measurements (points) of spectral D^* (500 K, f Hz, 1 Hz) of the bolometer (L = 10 mm, w = 10 μm, d = 1.7 μm, V_b = 9.0 V).

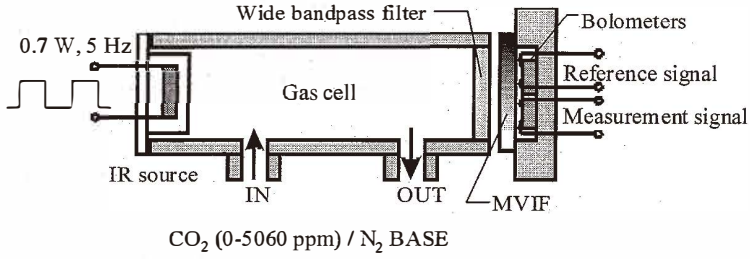

Fig. 12. Schematic diagram of the NDIR system.

filters consist of layers of film with ramped thickness. However, we adopted a structure that transforms the center wavelength by changing the thickness of only the spacer layer in the five-layer single halfwave (SHW) type filter as shown in Fig. 13. The MVIF experimentally produced offers continuous wavelength coverage from 3.8 μm and 4.3 μm. This wavelength range includes infrared absorption by CO_2. The MVIF was experimentally produced using a slit shutter sputtering system. The size of the MVIF was 1 cm^2. The spectral transmission of the MVIF measured by a spectrometer is shown in Fig. 14. The experiment results agree with the simulation for the characteristics of the spectral transmission. The linearity of the transmitted bands for different wavelengths at different measurement positions is within 1%. The cause of the 1% error is dispersion in the thickness of the film.

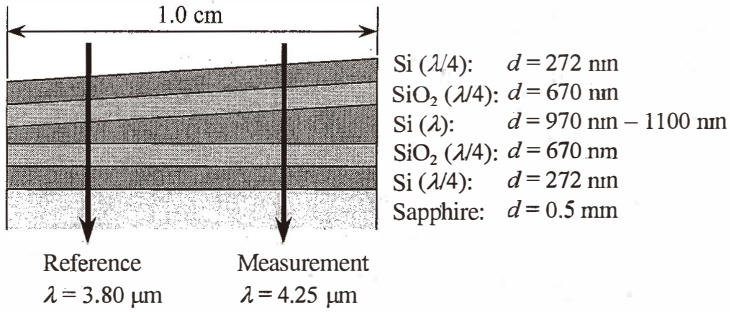

Fig. 13. Schematic diagram of the MVIF.

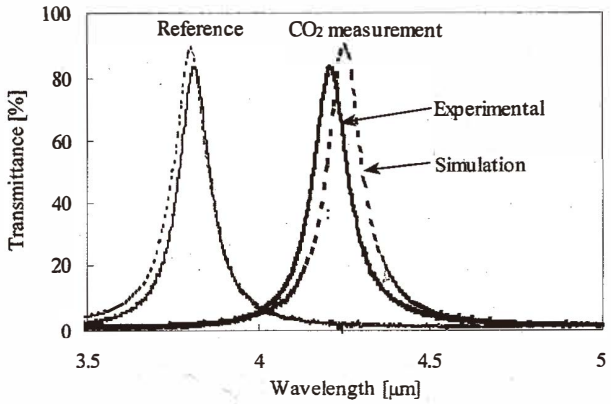

Fig. 14. Spectral transmission of the MVIF.

Signal output R_s of the bolometer for the reference wavelength ($\lambda = 3.8$ μm) and signal output M of the bolometer for the CO_2 measurement wavelength ($\lambda = 4.25$ μm) were measured at five values of CO_2 gas concentration in the range between 0 ppm to 5060 ppm. The relationship between the concentration of CO_2 and the signal of $\Delta M/R_s$ is shown in Fig. 15, where ΔM is the absolute value of the signal change from M_0 at 0 ppm concentration. The reproducibility of the measurement at 3σ was found to be within $\pm$ 3.6% of the measured value. These results demonstrate the possibility of using microfabricated CO_2 sensors for consumer and commercial installations.

7. Conclusions

We developed a bolometer fabricated of only highly boron doped single-crystal silicon. For optimizing the combination of TCR, electrical noise and absorptivity, a boron concentration of 1×10^{20} /cm^3 was selected. The bolometer was fabricated on an SOI wafer

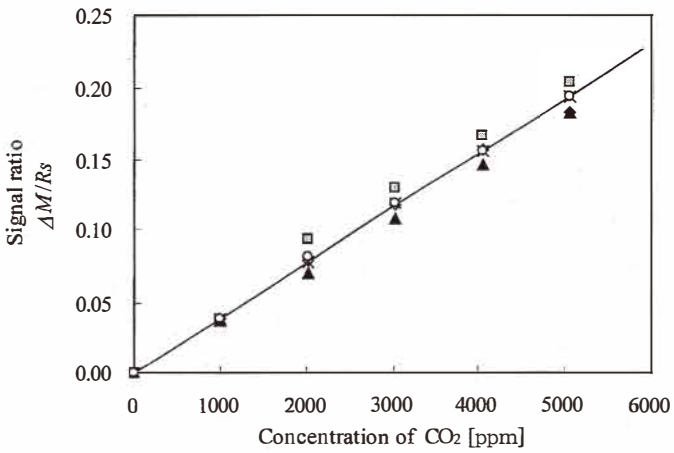

Fig. 15. Results of measurement of CO_2 concentration. R_s and M are the reference and measurement signal, respectively. $\Delta M = |M - M_0|$, where M_0 is the measurement signal at 0 ppm.

by bulk micromachining. The value of D^* (500 K, 10 Hz, 1 Hz) of the bolometer was measured to be 1.1×10^8 cmHz$^{1/2}$/W, which is in good agreement with the calculated value. Test measurements of CO_2 concentration by an NDIR system using two bolometers and the MVIF showed high reproducibility, which indicates good performance of the single-crystal silicon bolometers.

Acknowledgments

This work was performed under the management of Yokogawa Electric Corporation as a part of the R&D "Micromachine Technology" supported by the New Energy and Industrial Technology Development Organization (NEDO).

References

1 R. Lenggenhager, H. Baltes and T. Elbel: Sensors and Actuators A **37–38** (1993) 216.
2 P. W. Kruse: Uncooled IR Focal Plane Arrays, Proc. SPIE **2552** (1995) 556.
3 M. H. Unewisse, B. I. Craig, R. J. Watson, O. Reinhold and K. C. Liddiard: The Growth and Properties of Semiconductor Bolometers for Infrared Detection, Proc. SPIE **2554** (1995) 43.
4 C. N. Chen and J. S. Shie: Sensors and Materials **11** (1999) 369.
5 J. Y. W. Seto: J. Appl. Phys. **46** (1975) 5247.
6 H. Hara and H. Yamagishi: Micro Variable Infrared Filter, Trans. IEE of Japan **119**-E No. 2 (1999) 99.
7 F. N. Hooge: 1/f Noise Sources, IEEE Trans. Electron Devices **41** (1994) 1926.
8 J. S. Shie, Y. M. Chen, M. Ou-Yang and B. C. S. Chou: J. Microelectromechanical Systems **5** (1996).